THE ASTROPHYSICAL JOURNAL, 414:454–462, 1993 September 10

THE RADIAL VELOCITIES OF PLANETARY NEBULAE IN NGC 3379

ROBIN CIARDULLO[1,2]
Department of Astronomy and Astrophysics, Penn State University, 525 Davey Lab, University Park, PA 16802
GEORGE H. JACOBY
Kitt Peak National Observatory, National Optical Astronomy Observatories, P.O. Box 26732, Tucson, AZ 85726
AND
HERWIG B. DEJONGHE
Sterrenkundig Observatorium, Universiteit Gent, Krijgslaan 281-S9, B-9000 Gent, Belgium
Received 1993 January 12; accepted 1993 March 19

ABSTRACT

We present the results of a radial velocity survey of planetary nebulae (PNs) in the normal elliptical galaxy NGC 3379 performed with the Kitt Peak 4 m telescope and the NESSIE multifiber spectrograph. In two half-nights, we measured 29 PNs with projected galactocentric distances between 0.4 and 3.8 effective radii ($1 < R < 10$ kpc) with an observational uncertainty of ~ 7 km s^{-1}. These data extend 3 times further into the halo than any previous absorption-line velocity study. The velocity dispersion and photometric profile of the galaxy agrees extremely well with that expected from a constant mass-to-light ratio, isotropic orbit Jaffe model with $M/L_B \sim 7$; the best-fitting anisotropic models from a quadratic programming algorithm also give $M/L_B \sim 7$. The data are consistent with models that contain no dark matter within 3.5 effective radii of the galaxy's nucleus.

Subject headings: dark matter — galaxies: elliptical and lenticular, cD — galaxies: fundamental parameters — galaxies individual (NGC 3379) — planetary nebulae: general — techniques: radial velocities

1. INTRODUCTION

One of the outstanding problems in astronomy and astrophysics today is the question of how matter is distributed within galaxies. For spiral galaxies, we have gained some understanding of the mass distribution by using the 21 cm line of hydrogen to measure rotation curves. In comparison, very little is known about the mass distribution in elliptical galaxies. Because virtually all normal ellipticals possess a smooth luminosity profile, no emission features, and no neutral hydrogen, the kinematic study of these objects has usually been restricted to the central ~ 1 effective radius (r_e) where absorption-line measurements are possible. Hence, from the dynamical point of view, the outer half of these systems is almost completely unexplored. The best way to remedy this situation is to identify and measure individual test particles in the halos of these galaxies.

There are two classes of objects which can be used for this purpose: globular clusters and planetary nebulae (PNs). To date, globular clusters have been the more exploited. The halos of three large, early-type galaxies have been studied via globular cluster radial velocities: NGC 5128, M49 (NGC 4472), and M87. In the peculiar galaxy NGC 5128, Harris, Harris, & Hesser (1988) derived a mass-to-light ratio of $M/L_B \sim 17$ from observations of 87 globulars within a radius of ~ 20 kpc ($3.8r_e$). Mould et al. (1990) performed a similar experiment with 26 cluster velocities in the Virgo elliptical M49 and concluded that models with a massive, dark halo best fit the data, although a constant mass-to-light ratio of $M/L_B \sim 6.5$ was not ruled out. But perhaps the most interesting studies of globular cluster velocities have been those directed at M87 in the Virgo Cluster core (Mould, Oke, & Nemec 1987; Huchra & Brodie 1987; Mould et al. 1990). From the spectroscopy of 43 clusters with $r \lesssim 5r_e$, Mould et al. concluded that the mass-to-light ratio within 34 kpc of M87's nucleus is $M/L_B \sim 70$ and that a constant M/L with radius is ruled out. This kind of observation demonstrates the power of test particle radial velocity measurements for studying galactic halos.

Nevertheless, the use of globular clusters as dynamical probes in galaxies is somewhat limited. Once outside the Local Group, globular clusters are difficult to distinguish from faint foreground stars and background galaxies, and thus there is a significant amount of contamination in any list of candidates (cf. Sharples 1988; Mould et al. 1990). Moreover, because absorption-line spectra of faint objects are not conducive to radial velocity measurements, an enormous amount of effort must go into each individual measurement. These facts, along with a paucity of clusters in some nearby systems, have limited the use of globular clusters as dynamical probes to just a few objects.

Potentially, a more useful probe of galaxy kinematics is planetary nebulae. In the vast majority of galaxies closer than ~ 20 Mpc, there are far more PNs detectable than globular clusters, and, with an on-band/off-band filter technique, they are much easier to identify (cf. Ciardullo et al. 1989b; Jacoby, Ciardullo, & Ford 1990). Moreover, since PNs are emission-line objects, virtually every object that can be detected photometrically can also be measured spectroscopically. Since there is no trade-off between the precision of a PN velocity measurement and its signal-to-noise ratio as long as the emission line is unresolved ($R < 10{,}000$), an increase in spectroscopic dispersion serves only to decrease the sky noise and increase the velocity resolution. As a result, PN radial velocities can be

[1] Visiting Astronomer, Kitt Peak National Observatory, National Optical Astronomical Observatories, operated by the Association of Universities for Research in Astronomy, Inc., under contract with the National Science Foundation.
[2] NSF Young Investigator.

measured much more quickly and accurately than those of globular clusters.

Still, very few dynamical studies have involved planetary nebula observations. Although PNs have long been used to explore the stellar kinematics of the Magellanic Clouds (cf. Feast 1968; Webster 1969; Smith & Weedman 1972; Meatheringham et al. 1988), Lawrie's (1983) measurement of the stellar velocity dispersion in M31's bulge was the first application of their use in an early-type system. Shortly thereafter, Nolthenius & Ford (1986) analyzed the radial velocities of 15 planetaries in M32 and showed that the galaxy's stellar velocity distribution is almost certainly isotropic and that its global mass-to-light ratio is ~ 3. Nolthenius & Ford (1987) also used the radial velocities of 34 remote ($15 < R < 30$ kpc) planetaries in M31 to show that the rotation rate and velocity dispersion of M31's stellar halo is similar to that of its globular clusters. But the most comprehensive dynamical study so far has been the analysis of NGC 5128's halo planetary nebulae by Hui (1992, 1993). By measuring the radial velocities of 433 PNs with $r < 4r_e$, Hui showed that the stellar velocity field in NGC 5128 is distinctly triaxial, and that within 25 kpc ($\sim 4.5r_e$), the mass-to-light ratio of the galaxy is $M/L_B \approx 10$.

Unfortunately, planetary nebulae have not yet been used to explore the dynamics of a "normal" elliptical galaxy. M32 is a high surface brightness dwarf galaxy that has probably been tidally stripped (Faber 1973), and NGC 5128 is a peculiar elliptical with a dust lane, that is almost certainly undergoing a merger (Graham 1979). Neither of these galaxies can be called representative of the elliptical galaxy population.

Perhaps the best place to remedy this situation is in the normal, E0 galaxy NGC 3379. Positioned near the center of the Leo I group, the galaxy has been extensively examined photometrically to the extent that it has become a standard for surface photometry measurements (de Vaucouleurs & Capaccioli 1979; Lauer 1985a; Capaccioli et al. 1990). From the kinematical standpoint, the inner regions of the galaxy have also been extremely well studied: high-quality rotation and velocity dispersion profiles exist for the central $\sim 1'$ ($\sim 1.1r_e$) at six different position angles (Sargent et al. 1978; Davies 1981; Davies & Illingworth 1983; Davies & Birkinshaw 1988; Franx, Illingworth, & Heckman 1989). Moreover, NGC 3379 is one of the nearest normal elliptical galaxies, with a well-determined distance of ~ 10 Mpc from the planetary nebula luminosity function (Ciardullo, Jacoby, & Ford 1989a), the globular cluster luminosity function (Harris 1990), and the surface brightness fluctuation method (Tonry & Schneider 1989; Tonry 1991), and accurate positions exist for 93 PNs with radii between 0.3 and $4.1r_e$ (Ciardullo et al. 1989a). These data make the galaxy the ideal target for a dynamical study using planetary nebulae.

Here we present the results of a radial velocity survey of NGC 3379's halo planetary nebulae performed with the Kitt Peak 4 m telescope and the NESSIE multifiber spectrograph. In § 2, we describe our observations, estimate their accuracy, and present data for 29 PNs with galactocentric radii between $1 < R < 10$ kpc (0.4 and $3.8r_e$). In § 3, we combine these data with absorption-line measurements from the literature and give NGC 3379's velocity dispersion profile out to $\sim 3.5r_e$. We then compare this profile to model dispersions based on a Jaffe (1983) law and a King (1962) lowered isothermal potential and show that NGC 3379 resembles an isotropic-dispersion, constant mass-to-light ratio spheroid with $M/L_B \sim 7$. In § 4, we expand this analysis to anisotropic models, and again show that dark matter is not needed to fit the profile. We conclude by comparing our mass-to-light value with that derived for other galaxies and discussing the implications our data has for dark matter in other ellipticals.

2. OBSERVATIONS AND REDUCTIONS

On 1991 May 16 and 17 we observed the [O III] λ5007 emission lines of planetary nebulae in NGC 3379's outer envelope and halo with the bench-mounted R-C spectrograph and the NESSIE multifiber plugboard at the Cassegrain focus of the Kitt Peak 4 m telescope (Barden & Massey 1988). The specific instrument setup consisted of 36 blue-sensitive fibers (with an internal transmittance of $\sim 80\%$ at 5000 Å) and a 632 lines mm^{-1} grating blazed in first order at 5200 Å. The combination of this grating with NESSIE's 2".1 fibers and a Tektronix 1024 × 1024 CCD produced spectra with ~ 2.5 Å resolution and a dispersion of ~ 1.4 Å per pixel.

Unfortunately, not all of Ciardullo et al.'s (1989a) 93 PN candidates could be surveyed. Although in principle, we could have used NESSIE to observe 36 PNs at once, the minimum possible separation between any two fibers was 43". This constraint severely limited our choice of targets. Hence, on the first night, our observations consisted of two 1 hr exposures through a plugboard with fiber positions for 22 of NGC 3379's PNs. During this time, the seeing was 1".2. On the second night, which had somewhat worse (1".4) seeing, four 45 minute exposures were taken using a plugboard that contained the positions of 19 PNs in the galaxy. Since six planetaries were observed twice, these 5 hr of observations resulted in spectra for 35 objects.

The PN velocity measurements were accomplished using the IRAF data reduction package. After debiasing and flat-fielding the CCD frames, each spectrum was extracted from its parent image and wavelength calibrated in a ~ 400 Å region about 5007 Å using a helium-neon-argon comparison arc taken immediately before or after the observation. After rejecting obvious cosmic-ray events by visual inspection, the data from the multiple exposures were combined to create a net "summed" spectrum for each planetary. These spectra were then examined for the presence of [O III] λ5007 emission. In 29 of the 35 targets, the [O III] λ5007 line was clearly and unambiguously detected; for these objects, the redshift of λ5007 was determined by a Gaussian fit of the emission profile. A list of the detected PNs, along with their [O III] λ5007 wavelengths and heliocentric velocities appears in Table 1. Figure 1 displays the recorded spectra in the region between 4990 Å and 5060 Å. For reference, the mean velocity of the PN sample is 916 ± 22 km s^{-1}, in extremely good agreement with the galaxy's systemic velocity of 921 ± 27 km s^{-1} found by Davies & Birkinshaw (1988).

In order to estimate the accuracy of our velocity measurements, six planetary nebulae were observed on both NESSIE plugboards. A comparison of the velocities derived from the individual measurements appears in Table 2. The data show clearly that the velocity stability of the floor-mounted RC spectrograph was excellent. For four of the six PNs, the data taken on the two nights agree with each other to better than 0.1 Å, and the velocity error implied from the entire data set is $\sigma_{\rm err} \approx 7$ km s^{-1}. Considering that the PNs with multiple measurements are all at least 0.7 mag down the luminosity function and are among the faintest PNs observed, the true error is almost certainly not much larger than this.

TABLE 1

NGC 3379 PLANETARY NEBULA VELOCITIES

ID	Fiber Number		α(1950)	δ(1950)	m_{5007}	Radius	Velocity (km s^{-1})
	May 16	May 17					
1	12	...	10^{h}45^{m}13^s.67	12°50′34″.4	25.28	0.′63	936
2	48	...	10 45 12.94	12 51 22.0	25.33	0.76	1061
3	20	...	10 45 2.98	12 53 35.6	25.44	3.49	846
4	...	16	10 45 10.97	12 50 23.2	25.49	0.35	1015
5	...	35	10 45 12.21	12 51 13.9	25.51	0.56	1195
7	13	...	10 45 9.94	12 50 29.3	25.63	0.39	1060
8	24	...	10 45 9.73	12 51 46.4	25.65	1.10	713
13	41	...	10 45 19.42	12 50 9.1	25.77	2.09	911
15	43	...	10 45 22.94	12 50 1.7	25.77	2.96	965
16	...	47	10 45 13.88	12 51 56.0	25.78	1.37	832
17	25	...	10 44 59.88	12 50 44.5	25.81	2.75	818
19	22	...	10 45 6.74	12 51 8.0	25.83	1.15	716
21	33	...	10 45 3.61	12 48 37.6	25.86	2.80	831
22	23	...	10 45 17.06	12 50 58.5	25.91	1.46	704
25	47	...	10 45 7.77	12 53 57.8	25.95	3.33	992
26	21	...	10 45 2.01	12 52 29.1	25.96	2.84	933
27	39	...	10 45 10.52	12 49 31.5	25.96	1.22	985
29	...	31	10 45 6.70	12 50 50.9	25.99	1.10	977
38	...	14	10 45 17.01	12 50 41.5	26.14	1.42	1021
46	30	21	10 45 12.47	12 53 8.1	26.25	2.42	860
47	...	3	10 45 18.74	12 51 54.0	26.25	2.18	875
50	32	32	10 45 7.00	12 49 27.4	26.28	1.63	726
54	...	30	10 44 59.55	12 50 48.0	26.33	2.83	943
64	...	18	10 45 12.32	12 49 2.6	26.42	1.72	1091
69	35	33	10 45 3.02	12 50 15.4	26.48	2.04	836
71	19	48	10 45 16.23	12 52 47.5	26.48	2.40	1002
74	31	36	10 45 9.85	12 48 29.1	26.54	2.27	855
75	...	13	10 45 14.70	12 49 55.8	26.56	1.18	869
77	17	17	10 44 57.90	12 49 43.0	26.59	3.39	990

TABLE 2

PNs WITH MULTIPLE MEASUREMENTS

ID	m_{5007}	May 16 λ_{obs}	May 17 λ_{obs}	Δ Vel (km s^{-1})
46	26.25	5021.66	5022.09	26
50	26.28	5019.46	5019.52	4
69	26.48	5021.35	5021.25	6
71	26.48	5004.09	5024.15	4
74	26.54	5021.64	5021.67	2
77	26.59	5024.10	5023.73	22

3. THE HALO KINEMATICS OF NGC 3379

Although classified as an E0 galaxy in the Revised Shapley-Ames Catalog (Sandage & Tammann 1981), NGC 3379 appears slightly flattened on the sky, with an ellipticity of $b/a \approx 0.875$ and a major axis position angle of ~69° (de Vaucouleurs & Capaccioli 1979). This flattening is also evident in measurements of the rotation rate of the galaxy. Absorption-line analyses by Davies (1981), Davies & Illingworth (1983), Davies & Birkinshaw (1988), and Franx et al. (1989) have shown that although NGC 3379's central velocity dispersion is ~240 km s^{-1}, the galaxy does rotate slowly (~40 km s^{-1}) about its photometric minor axis. This has led Davies & Illingworth (1983) to suggest that the core of NGC 3379 is a rotationally flattened, isotropic-dispersion, constant mass-to-light ratio, oblate spheroid.

To see if this behavior extends to the outer portions of NGC 3379, we first examined our PN data for evidence of rotation in the galaxy's halo. Ordinarily, we would not expect to detect rotation from a sample of only 29 objects. Most dissipative collapse models of galaxy formation predict that the ratio of rotation to velocity dispersion, v/σ, should remain constant or decrease as one goes outward in a galaxy. Under these conditions, NGC 3379's rotation of $v/\sigma \sim 0.3$ should be undetectable with our small number of velocities. However, merger simulations show that encounters between galaxies can transfer angular momentum outward from a galaxy's inner regions to its halo (Barnes 1988). If so, then NGC 3379 might have a rapidly rotating halo, which could be detected in our data.

Figure 2 displays the PN velocities superposed on NGC 3379's luminosity contours. From the figure, it is immediately apparent that halo rotation is not an important part of the galaxy's kinematics. Within $1r_e$, NGC 3379 rotates about its photometric minor axis (position angle of 155°) with the southwest side of the galaxy receding. However, of the 24 PNs with projected radii, $r > 1r_e$, only 10 are moving in the direction of this rotation. At $r > 2r_e$, the story is the same—only six of 14 objects have a radial velocity consistent with minor axis rotation. In fact, there is no evidence in our data for significant rotation about any axis of the galaxy. Because our sample of objects is small, we cannot rule out the existence of an amount of rotation consistent with $v/\sigma \approx 0.3$. Nevertheless, a rapidly rotating halo does not exist in NGC 3379.

If we assume v/σ is negligible in NGC 3379's outer regions, we can estimate the halo velocity dispersion directly from the dispersion of our PN data. This is done in the upper portion of Figure 3, which groups the PNs into bins of nine, 10, and 10 objects. As a comparison, Figure 3 also displays azimuthally averaged absorption-line velocity dispersions derived from the observations of Sargent et al. (1978), Davies (1981), Davies & Illingworth (1983), and Davies & Birkinshaw (1988). (The

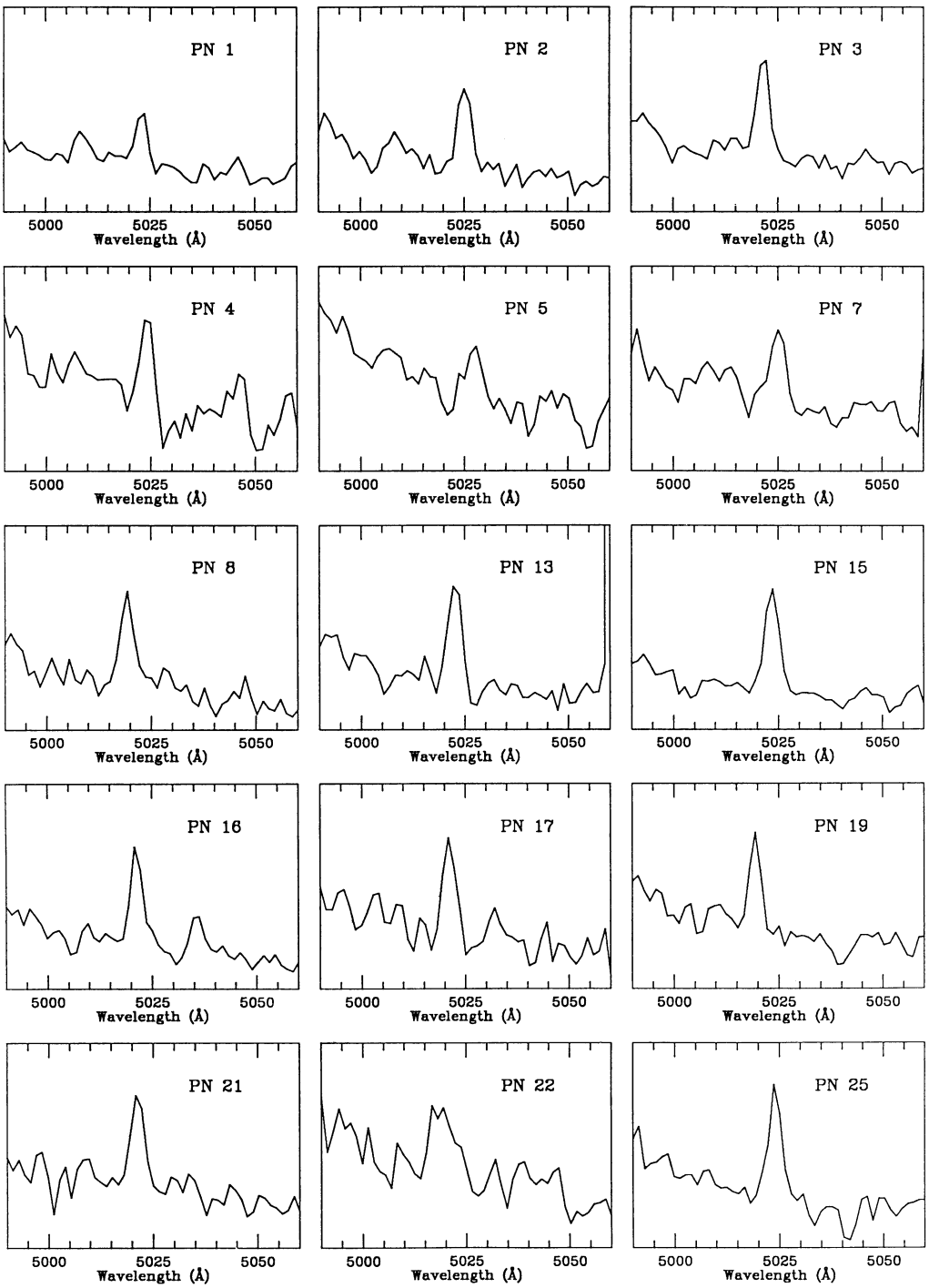

FIG. 1.—The spectra of 29 of NGC 3379's planetary nebulae in the wavelength region between 4990 and 5060 Å. The data have been debiased and flat-fielded, but not flux-calibrated. The [O III] λ5007 line is easily seen in every object.

Franx et al. 1989 dispersions are systematically lower by ~15% than those of the other groups and are not used in this calculation.) The plot shows that the stellar velocity dispersion in NGC 3379's halo declines with radius, as expected in a system without a massive halo.

Also displayed in the upper part of Figure 3 are the velocity dispersion profiles expected from Jaffe (1983) law [$\rho \propto r^{-2}(1+r)^{-2}$] galaxies with purely isotropic, circular, and radial orbits. Clearly, the models with radial and circular orbits do not fit the data and can be statistically excluded quite easily. If $\bar{v}$ is the systemic velocity of the galaxy, and $\sigma(r_i)$ is the quadratic sum of the measurement uncertainty and the model (Gaussian) velocity dispersion at radius r_i scaled by σ_0, then the sum over all planetaries

$$S^2 = \sum \left[\frac{(v_i - \bar{v})}{\sigma(r_i)} \right]^2 \quad (1)$$

is distributed as χ^2 and is a measure of goodness of fit (cf.

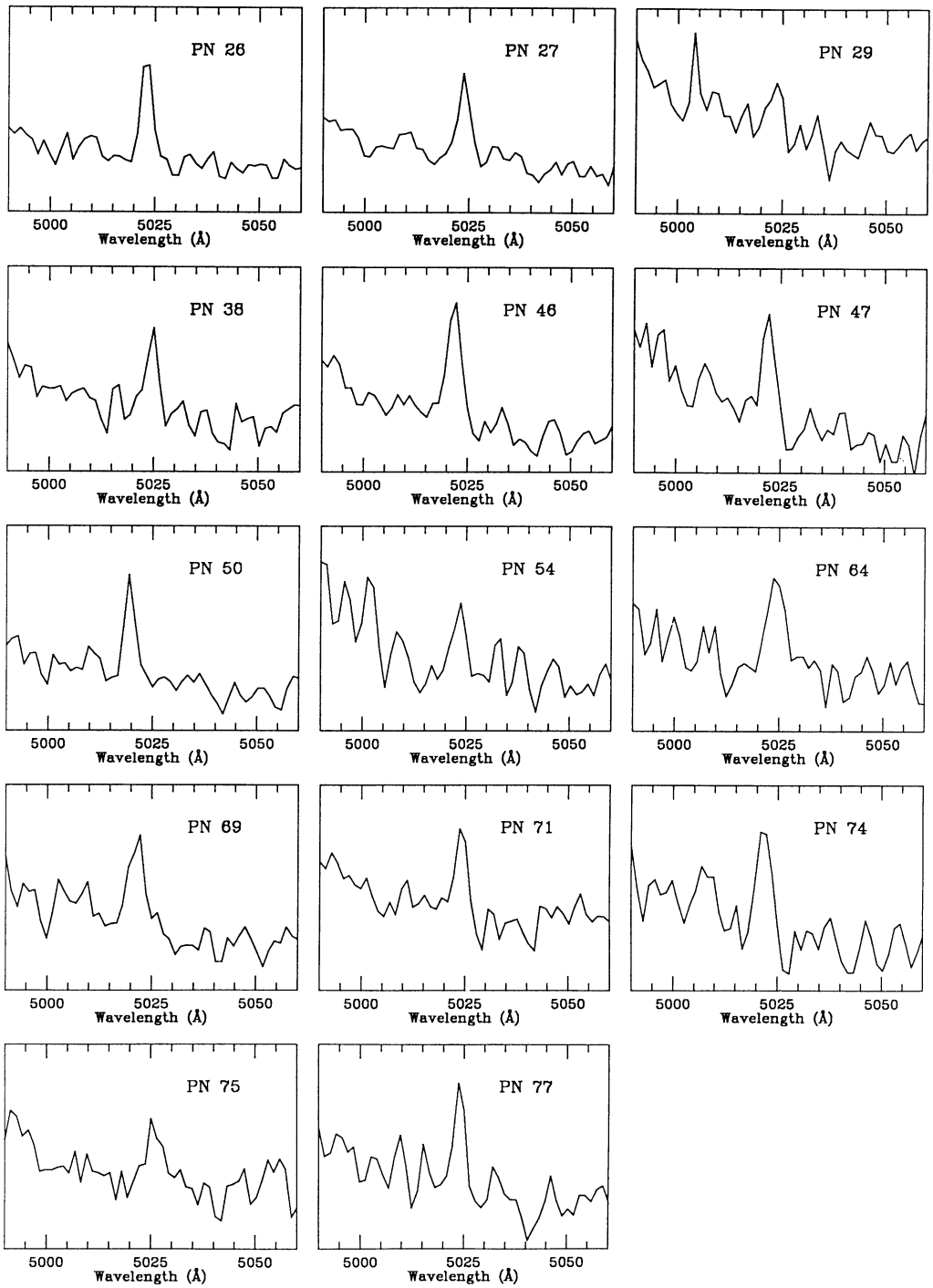

FIG. 1—*Continued*

Nolthenius & Ford 1986). For the case of purely radial orbits, the Jaffe model which best fits the absorption-line data has a reduced χ^2 from the planetaries of $\chi^2 = 4.21$, which, for 28 degrees of freedom, is excluded at the 99.9% confidence level. Similarly, if a circular orbit Jaffe model is fitted to the absorption-line dispersions, then the PN velocities give a reduced χ^2 of 0.55, which is excluded at better than a 98% level. In either case, it is obvious from the binned data that these nonisotropic models do not agree well with the observations.

On the other hand, Figure 3 demonstrates that NGC 3379's stellar kinematics are exceptionally well fitted by an isotropic orbit Jaffe model, or by a lowered isothermal King (1962) potential. When the absorption line measurements are used to constrain the Jaffe model, the PN data give a reduced χ^2 of

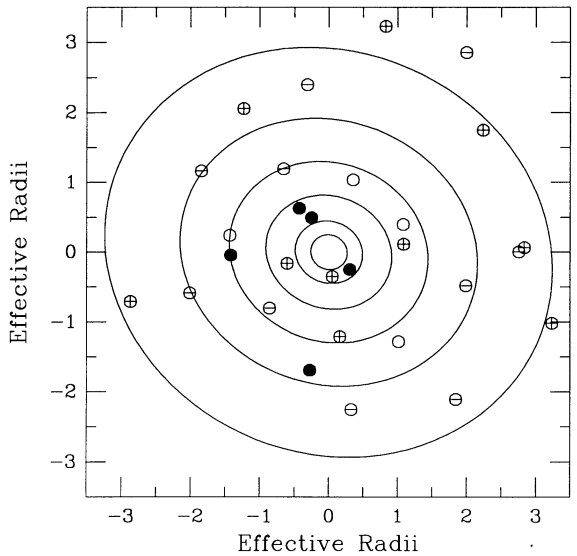

FIG. 2.—Displayed are NGC 3379's luminosity contours (at magnitude intervals, starting at $B = 20$) with the observed PNs superposed. North is at the top; east is to the left. The spatial scale is labeled in terms of the galaxy's effective radius, with $1r_e = 54''.8 = 2.7$ kpc. Filled circles represent objects that are receding with a galactic velocity greater than 100 km s^{-1}; inscribed plus signs denote PNs with $100 > v > 0$ km s^{-1}; inscribed minus signs show PNs with velocities $-100 > v > 0$ km s^{-1}, and open circles show objects with $v < -100$ km s^{-1}. The data show that rotation is not an important part of the PN kinematics at $r > r_e$. This is consistent with the 44 ± 5 km s^{-1} rotation about the photometric minor axis (west receding) found by Franx, Illingworth, & Heckman (1989) for $r < 0.5r_e$.

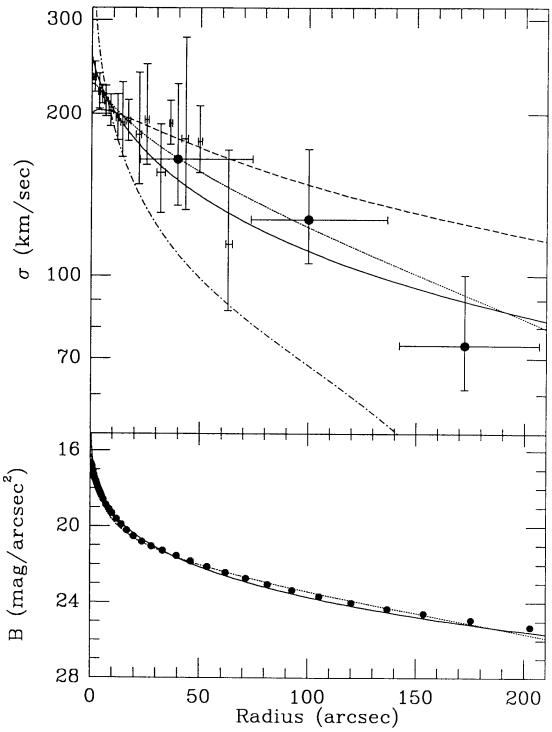

FIG. 3.—Displayed in the upper panel is the velocity dispersion profile for NGC 3379. The points are the azimuthally averaged absorption-line measurements from the literature; the filled circles are the PN velocity dispersion data, assuming no halo rotation. The error bars in x show the radii over which the data have been collected, while the errors in y represent 1 σ confidence intervals. The curves represent several constant mass/luminosity models, including a radial orbit Jaffe model (*dashes and dots*), a circular orbit Jaffe model (*dashes*), an isotropic orbit Jaffe model (*solid line*), and a log $r_t/r_c \sim 2.33$ isotropic King model (*dotted line*). The lower panel compares the Jaffe and King models' luminosity profiles with NGC 3379's B-luminosity profile derived from the surface photometry of de Vaucouleurs & Capaccioli (1979) and Lauer (1985a). The isotropic models are excellent fits to the data, and there is no evidence for the presence of dark matter in the galaxy.

0.998; if a $c = 2.33$ King law is used, the value of χ^2 is a very acceptable 0.85. The agreement between these two models and the PN measurements strongly suggests that the stellar orbits in NGC 3379 are isotropic and that dark matter is not important within $\sim 3.5r_e$ of the galaxy's nucleus.

If we assume that these constant mass-to-light ratio, isotropic orbit models accurately reflect NGC 3379's stellar distribution function, we can fit the models to the planetary nebulae and absorption-line data and obtain estimates of the galaxy's mass-to-light ratio. To do this, we start by computing the optimum scaling for the dispersion profiles via the method of maximum likelihood. For our sample of planetary nebulae with projected radii, r_i, and radial velocities, v_i, the model which best fits the data is that which maximizes the probability

$$P_{\rm PN} = \prod \left[\frac{1}{\sqrt{2\pi}\sigma(r_i)}\right] \exp\left\{-\frac{1}{2}\left[\frac{v_i - \bar{v}}{\sigma(r_i)}\right]^2\right\}. \quad (2)$$

Similarly, the best fit to the absorption line velocity dispersions is found by maximizing

$$P_{\rm abs} = \prod \exp\left\{\left[\frac{\sigma_{\rm obs} - \sigma(r_i)}{\epsilon_i}\right]^2\right\}, \quad (3)$$

where $\sigma_{\rm obs}$ is the observed velocity dispersion at radius r_i, and ϵ_i is the uncertainty in the measurement. When multiplied together, these two probabilities give the best estimate for the scaling parameter, σ_0, along with the uncertainty in the estimation.

Figure 4 shows the results from this maximum likelihood analysis for both the absorption line and planetary nebulae data. For the Jaffe model, the curves are in superb agreement. If we adopt $54''.8 \pm 3''.5$ as NGC 3379's effective radius (Capaccioli et al. 1990), then a fit of the PN data to the isotropic Jaffe model gives a most probable value for σ_0 of 361 km s^{-1}, with 68% of the probability lying between 322 and 422 km s^{-1}. When constrained by the absorption-line measurements, the best fit is nearly identical, although the uncertainty in the measurement is narrowed considerably, to $\sigma_0 = 367 \pm 8$ km s^{-1}. With an adopted distance of 10.1 ± 0.7 Mpc (Ciardullo et al. 1989a; Jacoby et al. 1992) and foreground absorption of $A_B = 0.05$ (Burstein & Heiles 1984), a luminosity-weighted fit of the Jaffe profile to the surface photometry of Lauer (1985a) and de Vaucouleurs & Capaccioli (1977) gives a global mass-to-light ratio for NGC 3379 of $M/L_B = 7.2 \pm 1.2$. The total mass implied by the law is $1.1 \times 10^{11}\, M_\odot$.

Although King models do not fit NGC 3379's photometric and kinematic data as well, the results implied by their use are similar. Lauer (1985b) has shown that the best-fitting King model for NGC 3379's central region has a core radius of $r_c = 1''.66 \pm 0''.07$ and a central surface brightness of $R_0 = 14.41 \pm 0.04$ mag arcsec^{-2}. With these parameters, and a concentration parameter of $c = 2.33$ (which fits the outer portions of the galaxy out to $r_e \sim 3.5$ moderately well), the planetary nebula observations give a most probable value for σ_0 of 208^{+35}_{-23} km s^{-1}. When both the PN and absorption-line measurements are fitted, $\sigma_0 = 229 \pm 5$ km s^{-1}. This velocity,

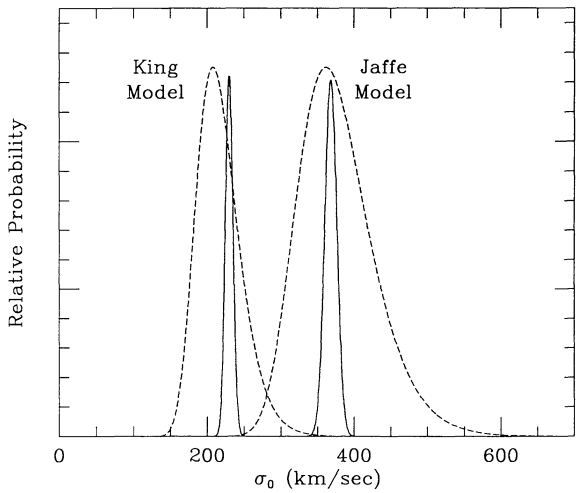

FIG. 4.—The results of the maximum likelihood fits of isotropic models to the absorption-line and planetary nebula velocity data. The abscissa is the scaling factor needed to fit the data; the ordinate is the relative probability of the model. The curves on the right are for an isotropic orbit Jaffe model with $r_j = 71''.8$, while the curves on the left are for a lowered isothermal (King) model with $\log r_t/r_c = 2.33$. The dotted lines are the relative probabilities for fitting the planetary nebula data alone; the solid lines show the fits to the absorption-line measurements. The almost perfect agreement for the two curves of the Jaffe model supports its use as a distribution function.

coupled with an assumed $(B-R)$ color of 2.21 (Lauer 1985b), gives a total galactic mass of $1.2 \times 10^{11}\ M_\odot$ and a most probable mass-to-light ratio of $M/L_B = 6.8 \pm 0.8$. This mass-to-light ratio is significantly greater than that of thermalized Galactic globular clusters (Illingworth 1976; Pryor et al. 1986; Mandushev, Spassova, & Staneva 1991), but well within the range measured in the interiors of normal spiral galaxies (Faber & Gallagher 1979).

4. A QP DYNAMICAL MODEL FOR NGC 3379

The above analysis assumes that the stellar orbits in NGC 3379 are entirely isotropic. However, it is quite possible that NGC 3379's stellar kinematics draws from some anisotropic distribution function. Since it is well known that mass estimates are dependent on the assumptions about the orbital structure, it is worthwhile to release the constraint of isotropic orbits and use the photometric and kinematic data together to produce a best possible model for NGC 3379's stellar distribution function.

Since NGC 3379 can be fitted with isotropic orbits, we cannot invoke any preconception on the anisotropy, since, if present, the anisotropy is likely to be rather small without a clear preference for either radially or tangentially biased orbits. Hence, to find the best-fitting model for the galaxy, we used a quadratic programming (QP) algorithm (Dejonghe 1989) which has the advantage of producing a best model in the following sense.

We assume that the stellar distribution function $F(E, L^2)$ depends on two integrals, binding energy E (per unit mass) and the modulus of the total angular momentum $L = |\boldsymbol{L}|$. Both the integrals E and EL^2 are always finite for bound orbits, and therefore a power series expansion of the form

$$F(E, L^2) = \sum_{i,j} a_{ij} E^{\alpha_i} (EL^2)^{\beta_j} \qquad (4)$$

is a reasonable and sufficiently general assumption. The functions $F_{i,j} = E^{\alpha_i}(EL^2)^{\beta_j}$ are essentially of the form first explored by Fricke (1952) and form a basis of a vector space of functions out of which we will pick a distribution function. This space is in fact an approximation of what in reality is a Hilbert space.

The QP algorithm determines the coefficients $a_{i,j}$ by minimizing a χ^2-type variable (which is a quadratic function of the coefficients), subject to the (linear) constraints that the distribution function must be everywhere positive in phase space. This χ^2-type variable can be constructed with whatever observational material is available as long as this information is linear in the distribution function, and it may sometimes even be given the usual statistical meaning.

In our case, we used luminosity densities $\rho_p(r_i)$ and pressures $\rho_p(r_j)\sigma_p^2(r_j)$, with $\sigma_p(r_j)$ the projected velocity dispersion. The photometry was taken from de Vaucouleurs & Capaccioli (1979) and is a perfect de Vaucouleurs profile. The data on the stellar kinematics were obtained by selecting from three sources: Davies & Birkinshaw (1988), Franx et al. (1989), and Davies & Illingworth (1983). The velocity dispersion profile for the PN sample was obtained by estimating the dispersion around the regression line through the radial velocity points as a function of radius, resulting in two data points at 80″ ($\sigma_p = 150\ \mathrm{km\ s^{-1}}$) and 200″ ($\sigma_p = 70\ \mathrm{km\ s^{-1}}$).

The integration of the Fricke components over all velocities depends on the potential. From the photometry, we calculated the spatial mass density and the potential by the well-known Abel inversion technique. The potential was then normalized so that the maximum binding energy was equal to one. This normalization is independent of the total mass of the system, which is accounted for by applying a suitable scaling to the kinematical data. Because the potential was derived entirely from the photometric data, all our models have a constant M/L.

The QP program was initialized by examining a large library of about 100 components and determining which two produced the best fit to the photometric data alone. These two components typically represent a core and a halo of the population. To this best pair, we then added additional components from the same library, now using both the kinematical and photometric data in the selection process. By following this prescription, we were able to obtain very acceptable fits to the data with only ~ 15 components.

It turns out that there are many models possible that all fit the photometry and the kinematical data. In order to illustrate this, we present in Figure 5 a $1 \times 10^{11}\ M_\odot$ model which was forced to be radial in the range 11–13 kpc, with $\sigma_r/\sigma_\varphi \geq 1.5$. This can be done easily in the QP algorithm, since the condition simply translates into a few additional constraints. We remark that the model is completely radial. On the other hand, one can also produce more complicated models, such as presented in Figure 6. That model again has a mass of $1 \times 10^{11}\ M_\odot$ but was forced to be tangential in the same range with $\sigma_r/\sigma_\varphi \leq 0.75$, and radial in the range 1–3 kpc, with $\sigma_r/\sigma_\varphi \geq 1.5$. Note that in the center all these models must be isotropic. Not surprisingly, the outermost values for σ_p are somewhat higher than in the purely radial model.

A general feature of the models is the very good fit to the photometry. This is purposely obtained, since the surface density is the zeroth-order moment of the line-of-sight velocity distribution, and therefore provides the normalization needed to convert pressures to velocity dispersions. Note also that a de Vaucouleurs profile can be reproduced with a relatively small number of Fricke-type components.

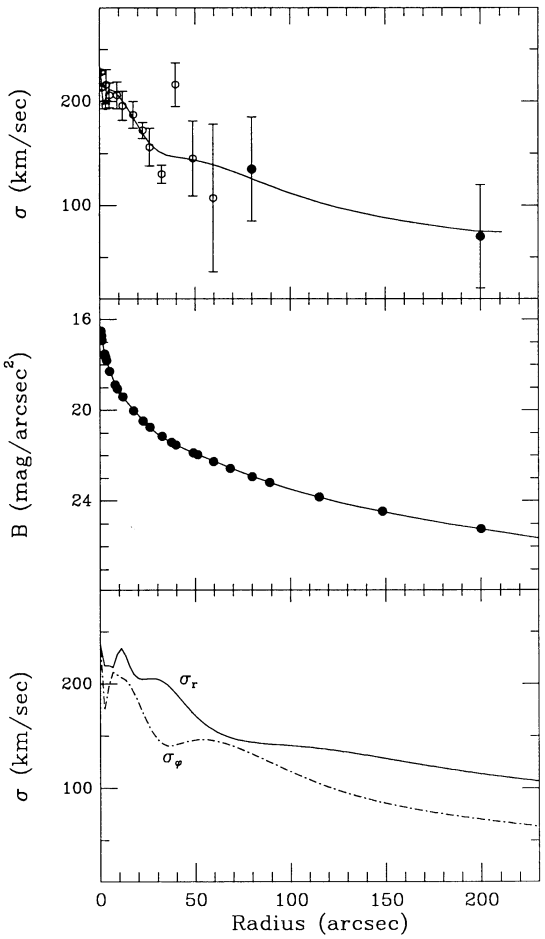

FIG. 5.—The velocity dispersion (*upper panel*) and luminosity profile (*middle panel*) of NGC 3379 along with an anisotropic, constant $M/L_B = 7$ QP model. In the velocity dispersion plot, open circles represent absorption-line velocity dispersions, while the planetary nebula data are displayed as solid points. The good fit demonstrates that a dark matter component is not needed to fit the data. The lower panel shows the radial and tangential (spatial) velocity dispersions. The model was forced to be radial in the 11–13 kpc range.

It is important to note, however, that the radial velocity data extend to about 10 kpc, and beyond that radius, the model is not constrained, save for the photometry. Again, the agreement between the models and the data show that there is no particular reason to invoke dark matter with the QP fit.

5. DISCUSSION

Our radial velocity measurements strongly argue that there is little dark matter associated with NGC 3379. However, this observation does not mean that there is no dark matter in the vicinity. NGC 3379 and its SB0 companion NGC 3384 are surrounded by a $\sim$200 kpc radius ring of neutral hydrogen which may be in a Keplerian orbit about the system (Schneider et al. 1989; Schneider 1989, 1991). If so, the total mass of the NGC 3379/3384 system is $\sim 6 \times 10^{11}\ M_\odot$ and the implied mass-to-light ratio is $M/L_B \sim 27$. Although this value for M/L is within a factor of $\sim$4 of our measurement, and much less than that estimated for spiral and dwarf spheroidal galaxies, it does leave a substantial amount of mass unaccounted for. Either this mass is associated with NGC 3384, or the entire NGC 3379/3384 system may lie in a dark matter halo.

Is the absence of dark matter within $\sim 3.5 r_e$ of NGC 3379 unusual? In general, the evidence for dark matter in early-type systems is mixed. While the globular cluster velocities provide strong support for the presence of a dark halo around M87, the case is not as clear-cut for normal members of the population. Based on the extended velocity dispersion profiles of NGC 4472, NGC 7144, and IC 4296 (which in some cases extend out to more than $2r_e$) and the dispersion profiles of NGC 1400, NGC 4946, NGC 5812, NGC 6721, NGC 7507, and NGC 7796 (Bertin et al. 1989), Saglia et al. (1993) argue that there exist two classes of ellipticals. Ellipticals of the first class have decreasing dispersion profiles and do not need dark matter to explain their dynamics, while ellipticals of the second class show nearly constant (or, in the case of NGC 7144, even rising) velocity dispersion profiles and are more likely to be dark matter candidates. If this is correct, NGC 3379 would belong to the first class, with little or no dark matter.

In a few ellipticals, the presence of an H I disk can be used to probe the matter distribution within several r_e; in most (but not all) of those cases, dark matter is again found to be unimportant (Kent 1990). But for most ellipticals, the only estimator of halo mass comes from the observation of X-ray gas. From the X-ray luminosity profile of normal ellipticals, several groups have concluded that these galaxies have high dynamical masses, with mass-to-light ratios of $\sim$50 (Forman, Jones, & Tucker 1985; Fabian et al. 1986). However, these results

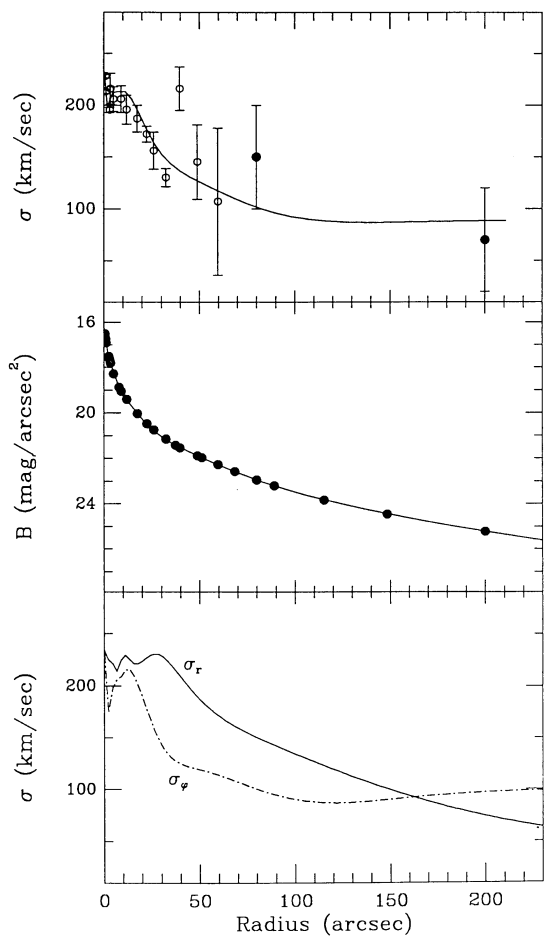

FIG. 6.—Same as Fig. 5, but for a model that was forced to be tangential in the 11–13 kpc range and radial in the 1–3 kpc range.

depend critically on the temperature profile of the gas, so in most cases, the uncertainties still allow models with little or no dark matter (Trinchieri, Fabbiano, & Canizares 1986; Fabbiano 1989). Thus, again, it is quite possible that NGC 3379, with its lack of dark matter, is representative of its class.

One possible explanation for the absence of dark matter around NGC 3379 comes from its location near the center of the Leo I group. Numerical simulations suggest that, in the process of forming a cluster, the massive halos of galaxies can be stripped away (West & Richstone 1988). Evidence in support of this scenario has been presented by Whitmore, Forbes, & Rubin (1988), who found that spirals near the centers of clusters have flat or falling rotation curves, while spirals in the outer regions of clusters have flat or rising curves. If such is the case, the halo of NGC 3379 may have been stripped off in the distant past.

6. CONCLUSIONS

While there is an abundance of evidence for dark matter in spiral and dwarf spheroidal galaxies, the very few studies of normal, noncentral ellipticals have produced mixed results on this issue. We have tested for the presence of dark matter in the nearby elliptical NGC 3379 by using halo planetary nebulae as test particles and measuring their radial velocities. The kinematics of the PNs suggest that the stellar orbits in NGC 3379's halo are likely to be isotropic and are not significantly influenced by dark matter. The implication is that either NGC 3379's dark matter halo has been stripped off during past galactic encounters, or that dark matter is not as important for elliptical galaxy dynamics as it is for spirals and dwarf spheroidals.

Because it is relatively easy to identify unambiguously halo planetary nebulae and to measure accurately their radial velocities, PNs provide a powerful tool for examining the kinematics of the stellar populations in galaxies of all Hubble types. The analysis of PNs in NGC 3379 represents a step in this direction.

This research has made use of the NASA/IPAC Extragalactic Database (NED) which is operated by the Jet Propulsion Laboratory, California Institute of Technology, under contract with the National Aeronautics and Space Administration.

REFERENCES

Barden, S. C., & Massey, P. 1988, in Fiber Optics in Astronomy, ed. S. C. Barden (ASP Conf. Ser., 3), 140
Barnes, J. E. 1988, ApJ, 331, 699
Bertin, G., et al. 1989, ESO Messenger, 56, 19
Burstein, D., & Heiles, C. 1984, ApJS, 54, 33
Capaccioli, M., Held, E. V., Lorenz, H., & Vietri, M. 1990, AJ, 1813
Ciardullo, R., Jacoby, G. H., & Ford, H. C. 1989a, ApJ, 344, 715
Ciardullo, R., Jacoby, G. H., Ford, H. C., & Neill, J. D. 1989b, ApJ, 339, 53
Davies, R. L. 1981, MNRAS, 194, 879
Davies, R. L., & Birkinshaw, M. 1988, ApJS, 68, 409
Davies, R. L., & Illingworth, G. 1983, ApJ, 266, 516
de Vaucouleurs, G., & Capaccioli, M. 1979, ApJS, 40, 699
Dejonghe, H. 1989, ApJ, 343, 113
Fabbiano, G. 1989, ARA&A, 27, 87
Fabian, A. C., Thomas, P. A., Fall, S. M., & White, R. E. 1986, MNRAS, 221, 1049
Faber, S. M. 1973, ApJ, 179, 423
Faber, S. M., & Gallagher, J. S. 1979, ARA&A, 17, 135
Feast, M. W. 1968, MNRAS, 140, 345
Forman, W., Jones, C., & Tucker, W. 1985, ApJ, 293, 102
Franx, M., Illingworth, G., & Heckman, T. 1989, ApJ, 344, 613
Fricke, W. 1952, Astron. Nach., 280, 193
Graham, J. A. 1979, ApJ, 232, 60
Harris, W. E. 1990, PASP, 102, 966
Harris, H. C., Harris, G. L. H., & Hesser, J. E. 1988, in IAU Symp. 126, Globular Cluster Systems in Galaxies, ed. J. E. Grindlay & A. G. D. Philip (Dordrecht: Kluwer), 205
Huchra, J., & Brodie, J. 1987, AJ, 93, 779
Hui, X. 1992, Ph.D. thesis, Boston Univ.
———. 1993, in IAU Symp. 155, Planetary Nebulae, ed. R. Weinberger & A. Acker (Dordrecht: Kluwer), in press
Illingworth, G. 1976, ApJ, 204, 73
Jacoby, G. H., et al. 1992, PASP, 104, 599
Jacoby, G. H., Ciardullo, R., & Ford, H. C. 1990, ApJ, 356, 332
Jaffe, W. 1983, MNRAS, 202, 995
Kent, S. M. 1990, in Evolution of the Universe of Galaxies, ed. R. G. Kron (ASP Conf. Ser., 10), 109
King, I. R. 1962, AJ, 67, 471
Lauer, T. R. 1985a, ApJS, 57, 473
———. 1985b, ApJ, 292, 104
Lawrie, D. G. 1983, ApJ, 273, 562
Mandushev, G., Spassova, N., & Staneva, A. 1991, A&A, 252, 94
Meatheringham, S. J., Dopita, M. A., Ford, H. C., & Webster, B. L. 1988, ApJ, 327, 651
Mould, J. R., Oke, J. B., de Zeeuw, P. T., & Nemec, J. M. 1990, AJ, 99, 1823
Mould, J., Oke, J. B., & Nemec, J. 1987, AJ, 93, 53
Nolthenius, R., & Ford, H. 1986, ApJ, 305, 600
———. 1987, ApJ, 317, 62
Pryor, C., McClure, R. D., Fletcher, J. M., & Hesser, J. E. 1986, in IAU Symp. 126, Globular Cluster Systems in Galaxies, ed. J. E. Grindlay & A. G. D. Phillip (Dordrecht: Kluwer), 661
Saglia, R. P., et al. 1992, ApJ, 403, 567
Sandage, A., & Tammann, G. A. 1981, A Revised Shapley-Ames Catalog of Bright Galaxies (Washington: Carnegie Institution of Washington)
Sargent, W. L. W., Young, P. J., Boksenberg, A., Shortridge, K., Lynds, C. R., & Hartwick, F. D. A. 1978, ApJ, 221, 731
Schneider, S. E. 1989, ApJ, 343, 94
———. 1991, in Warped Disks and Inclined Rings around Galaxies, ed. S. Casertano, P. D. Sackett, & F. H. Briggs (Cambridge: Cambridge Univ. Press), 25
Schneider, S. E., et al. 1989, AJ, 97, 666
Sharples, R. M. 1988, in IAU Symp. 126, Globular Cluster Systems in Galaxies, ed. J. E. Grindlay & A. G. D. Philip (Dordrecht: Kluwer), 545
Smith, M. G., & Weedman, D. W. 1972, ApJ, 177, 595
Tonry, J. L. 1991, ApJ, 373, 1
Tonry, J., & Schneider, D. P. 1989, AJ, 96, 807
Trinchieri, G., Fabbiano, G., & Canizares, C. R. 1986, ApJ, 310, 637
Webster, B. L. 1969, MNRAS, 143, 97
West, M. J., & Richstone, D. O. 1988, ApJ, 335, 552
Whitmore, B. C., Forbes, D. A., & Rubin, V. C. 1988, ApJ, 333, 542